PERGAMON

International Journal of Heat and Mass Transfer 41 (1998) 4205–4228

International Journal of HEAT and MASS TRANSFER

Two-phase co-current flow in inclined pipe

P. L. Spedding*, J. K. Watterson, S. R. Raghunathan, M. E. G. Ferguson

Department of Aeronautical Engineering, The Queen's University of Belfast, David Keir Building, Stranmillis Road, Belfast BT9 5AG, N. Ireland

Received 3 January 1998; in final form 18 March 1998

Abstract

Data are presented on horizontal and slightly inclined flows at $+5$ and -5° for a 0.058 m inner diameter (i.d.) pipe with the co-current air–water system.

The prediction capabilities of existing flow regime maps were shown to be inadequate. However, the transitions for stratified ripple to role wave, for slug to blow-through-slug, for film plus droplet to stratified, and the modified maps for stratified type to slug flows all gave good prediction performance with horizontal and slightly inclined flows.

The largest liquid hold-up occurred in upward flow except at high gas rates and low liquid rates where the downflow condition gave the highest liquid hold-up. The lowest liquid hold-up occurred in downward flow at low gas flow rates and horizontal flow at high gas flow rates. Hold-up prediction proved to be flow regime dependent.

The inclined total average pressure drop data crossed over the horizontal data from higher to lower values with increasing gas rate at a gas rate of just under $\bar{V}_{SG} = 10$ m s^{-1}.

Below this gas rate the horizontal pipe gave the lowest pressure drop while above this gas rate the upwardly inclined pipe gave the lowest pressure drop. A pressure loss minimum occurred at $\bar{V}_{SG} = 10$ m s^{-1} for upward flows. Below $\bar{V}_{SG} = 10$ m s^{-1} the pressure loss for downward flow was virtually independent of gas rate being mainly due to hydrostatic head. As the gas flow approached $\bar{V}_{SG} = 50$ m s^{-1} there was very little effect of inclination on the pressure loss.

Pressure drop was successfully predicted although the accompanying hold-up prediction was not always reliable.

Nomenclature

d diameter
g gravitational constant [m s^{-2}]
H heaviside functions equation (3)
N_{GV} gas velocity number, $\bar{V}_{SG}(\rho_L/g\sigma)^{1/4}$
N_{LV} liquid velocity number, $\bar{V}_{SL}(\rho_L/g\sigma)^{1/4}$
Fr Froude number, $(\bar{V}_T/\sqrt{gd})^{1/2}$
Q flow rate [m^3 s^{-1}]
$\bar{R}$ holdup
$\bar{V}$ velocity [m s^{-1}].

Greek symbols
α angle degrees
ρ density [kg m^{-3}]
σ surface tension [kg s^{-2}].

Subscripts
G gas
L liquid
S superficial
T total.

1. Introduction

Traditionally, production from oil/gas wells has been separated locally into its various constituents and the products subsequently transported separately in, for example, pipelines to processing facilities. A more attractive alternative strategy that is finding increasing use with offshore installations is to handle the well head fluids multiphase in an appropriate distribution system that is laid to broadly coincide with the prevailing terrain. The multiphase pipeline would follow the general dips and rises of the sea floor finally rising up to the onshore facilities. In general, multiphase flow exhibits a greater

* Corresponding author.

0017–9310/98 $19.00
PII: S0017–9310(98)00122–7

pressure loss than the corresponding single phase condition although drag reduction phenomena exist [1]. In addition small departures from horizontal geometry affect the flow characteristics. One of the major consequences being that, unlike single phase flow, the hydrostatic component of pressure drop usually will not be recovered between uphill and downhill flow sections of pipe. Of the 50 or so papers that have appeared on the subject of two-phase flow close to horizontal conditions only three sets of data have given a comprehensive coverage of the geometric and the two-phase characteristics involved [2–8]. Even then the data were not always collected in an appropriately systematic manner that allowed clear evaluation of the trends. For example, the liquid rate [2–4] and the inclination [5–7] were not controlled properly. Despite these problems a number of models have been formulated for prediction of two-phase phenomena in inclined flows. Two problems are apparent. The first rises out of the existing data which shows anomalous effects around the horizontal. The second concerns the design of fluid piping systems. Some designs suggest that systems should be as close to horizontal as possible while others suggest that in order to facilitate drainage of the pipe it should slope downwards slightly in the flow direction. However, field experience has sometimes cast doubt on the wisdom of this design. The main purpose of this work is to cast light on these problems.

Flow patterns, hold-up and pressure loss data were obtained for co-current air–water flow (max rate 0.135 m s^{-1} at 1.05 bar (a) and 0.003 m s^{-1} respectively) in a 0.0508 m (i.d.) perspex pipe at angles of -5, 0 and $+5^{\circ}$. The design and operation of the equipment was checked and validated to ensure results were reliable and reproducible. Details are given elsewhere [9].

2. Results and discussion

2.1. Regime maps

All existing flow regime maps have been tested against data obtained here and elsewhere [10, 11]. In a number of aspects each of the maps have been found to be inadequate. The following discussion is not intended to be all inclusive but highlights relevant aspects to indicate the current state of the art.

2.1.1. Taitel–Dukler map

The map is presented in Fig. 1. The transition prediction for horizontal flow between smooth stratified and stratified plus wavy flow was shown to be poor. However, Andritos and Hanratty [13] were able to predict the stratified plus ripple transition with a better degree of accuracy by substituting a value of 0.06 for s, the sheltering coefficient. Even so, the predicted transition was far from satisfactory at low liquid velocities. Taitel and Dukler [12] did not distinguish between the various stratified wavy regimes and the film plus droplet pattern, but instead assigned a hybrid stratified-wavy region on their map making it deficient in this respect. The transition between stratified type flows and the slug regime was found to give fair prediction which tended to deteriorate as the pipe diameter rose. Taitel and Dukler [12] showed that discrepancies between the Weisman et al. [15] data and the proposed transition method were due to the use of a short pipe length. A modification to their original theory was proposed that included pipe length as a parameter for the transition to slug flow. Similarly, the accuracy of the predicted transition from stratified wavy to annular flow was found to deteriorate as the pipe diameter increased, with more film plus droplet observations being located in the annular region of the map. Transitions from slug to annular flow are also shown in Fig. 1. The Taitel and Dukler [12] criterion predicted the transition from slug to blow-through-slug patterns with better precision. Kokal and Stanislav [8] reported that the blow-through-slug pattern, which fell on the transition between slug and wavy annular flow, was difficult to identify since a problem existed in distinguishing visually between highly aerated slugs and the annular plus roll wave flow patterns. This difficulty was overcome in this work by cross reference to the pressure fluctuations which clearly identified the transition. Kokal and Stanislow [8] defined the transition from slug to annular flow which was found to demarcate well between the slug and blow-through-slug regimes for the three pipe diameters of 0.0454, 0.0508 and 0.0935 m.

The Barnea and Taitel [16, 17] map followed a very similar pattern to the Taitel and Dukler [12] map. The inclined data were even more at variance with these suggested maps.

2.1.2. Mukherjee and Brill map

Figure 2 shows the flow pattern map developed by Mukherjee and Brill [4] tested against data. For horizontal flow, the map under-predicted the stratified to annular boundary. This under-prediction caused problems with the slug to annular boundary which traversed the blow-through-slug regime. The bubble to slug demarcation was also inaccurate.

The upflow map also did not handle the blow-through-slug regime, but the slug to annular boundary gave a more realistic result than for horizontal flow. For downflow, the dominance of stratified type flows was not reflected by the map. Hence the bubble to slug and slug to annular transitions were unrealistic. The stratified to annular transition was again underpredicted in a similar manner to horizontal flow.

2.1.3. Spedding and Nguyen map

The empirical flow pattern map proposed by Spedding and Nguyen [5] for horizontal flow were compared with

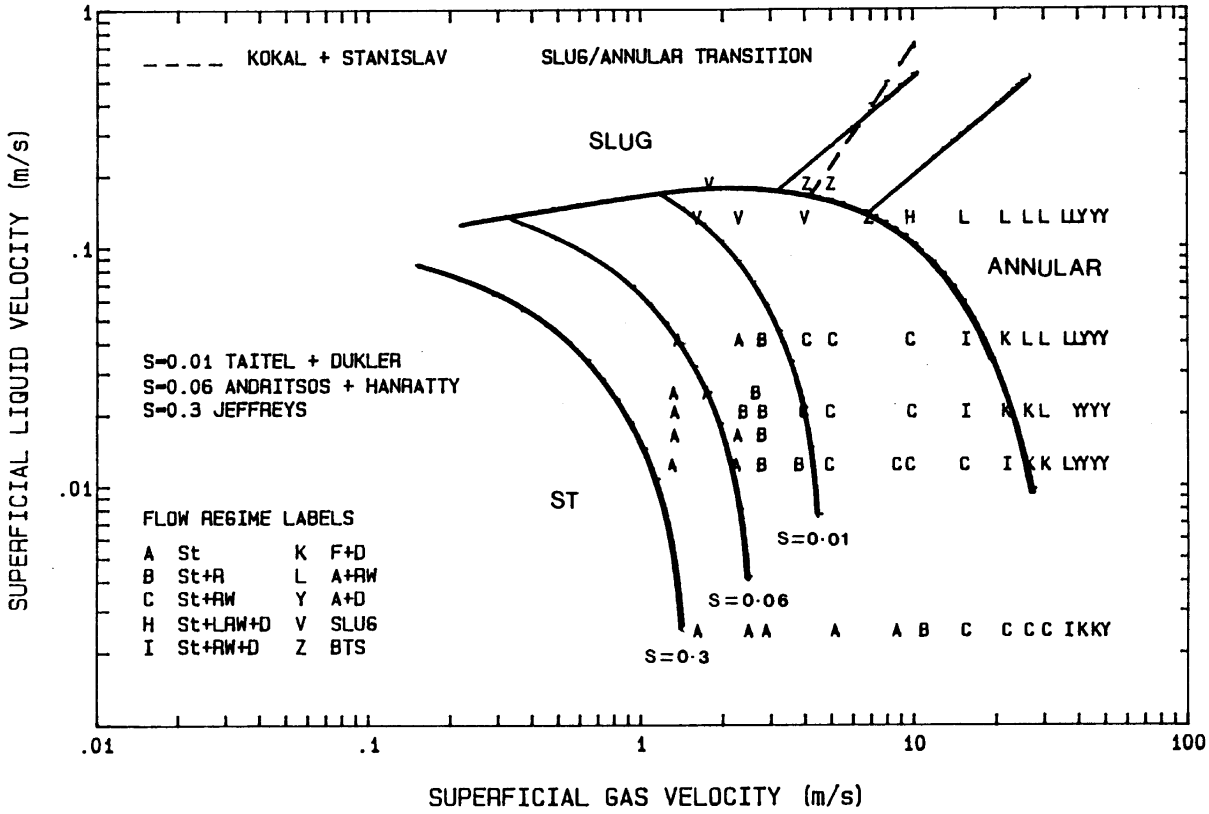

Fig. 1. The Taitel and Dukler [12] map compared to the horizontal air–water data for 0.0508 m (i.d.) pipe.

the data obtained for three different diameters. The transition from slug flow to the stratified regions was predicted satisfactorily but pipe diameter had a significant effect on the accuracy of certain of the other flow regime transitions. The assumption that liquid droplets did not exist in the gas core during horizontal annular flow was unfounded and the annular flow patterns were more properly assigned with the mixed flow patterns where both phases were discontinuous. Figure 3 details a suggested modification of the horizontal map which exhibited better agreements with data for all diameters.

Discrepancies also appeared in the flow pattern maps proposed by Spedding and Nguyen [5] for inclined flows when compared with data from this work. The transition from stratified to slug flow in slightly inclined up-flow was inaccurate since slug flow was present, at least initially, for all liquid flow rates requiring that the slug flow regime should therefore cover a much larger area of the map than suggested by Spedding and Nguyen [5]. Figure 4 shows the suggested map for inclined flow at $+5^{\circ}$. The map possessed significant differences to the horizontal case. However, the only difference between $+2.75^{\circ}$ data [10] and the $+5^{\circ}$ data of this work was that the slug to stratified roll wave and blow-through-slug transitions rose as the angle was increased. Figure 5 shows the suggested map for downward inclined flow at -5°, which showed minor differences to the Spedding and Nguyen [5] equivalent.

2.1.4. Transition criteria

The theoretical flow pattern criteria of Weisman et al. [15] were compared against data as shown in Fig. 6. The transition from stratified to slug flow over estimated the experimental data in all cases. The transition from smooth stratified to wavy flow gave good prediction for all pipe diameters. The transition to annular flow underestimated the experimental data in all cases. Figure 6 shows some film plus droplet observations in the annular region of the map. Although Weisman et al. [15] used pipelines of different diameters, the maximum was 0.051 m (i.d.). The transition to annular flow was found by Lin and Hanratty [18] to occur by two mechanisms which depended upon the pipe diameter. Annular flow was found to develop at lower gas velocities by a mechanism of wave wrapping in a 0.0252 m (i.d.) pipeline, compared to an annular flow droplet deposition mechanism in a 0.0953 m (i.d.) pipeline. These findings may explain the

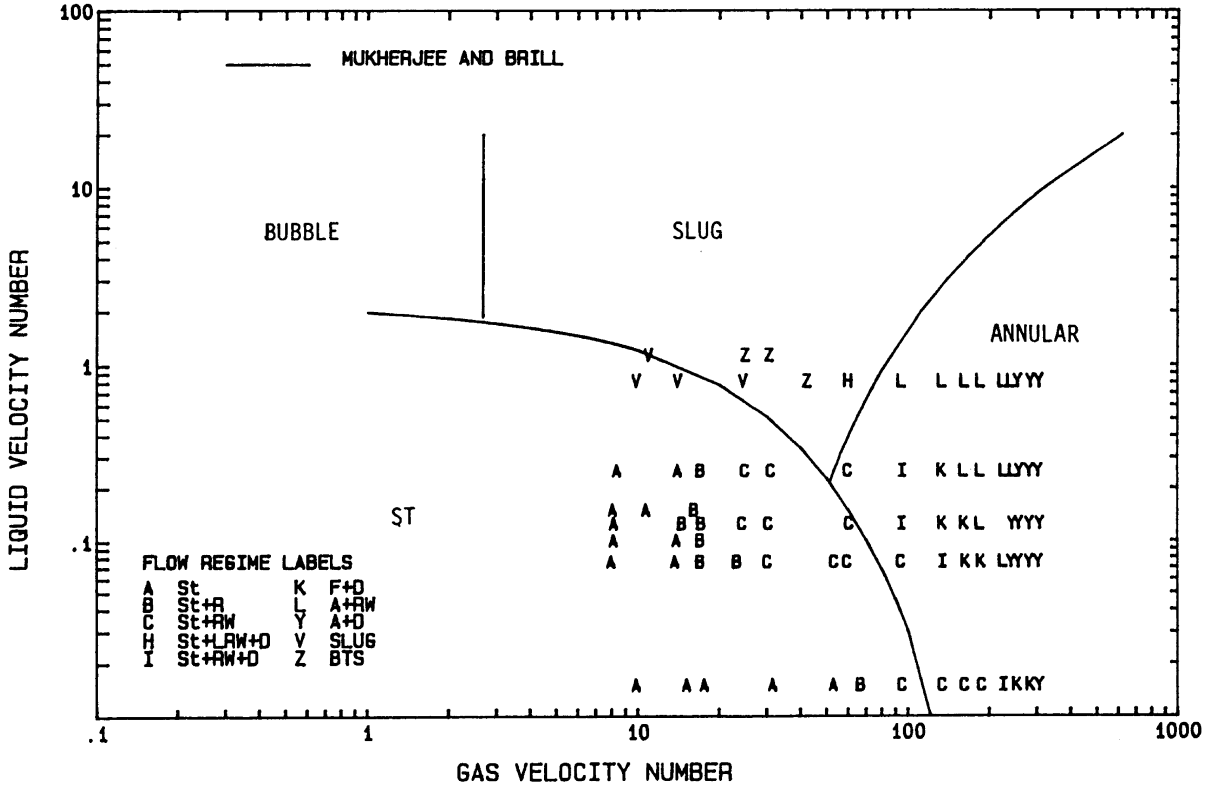

Fig. 2. The Mukherjee and Brill [4] map compared to the horizontal air–water data for 0.0508 m (i.d.) pipe.

occurrence of film plus droplet observations in the Weisman et al. [15] annular region.

The entrainment transition criteria of Ishii and Grolmes [19, 20] is also shown in Fig. 6 and gave excellent prediction of the transition to entrained stratified flows for all pipe diameters. The Kowalski [21] transition also showed good prediction between the stratified ripple and roll wave pattern.

2.2. Holdup

Figure 7 shows hold-up results for horizontal flow. The data present as a logarithmic series of straight lines with azympotic limiting values of $\bar{R}_L$ at both low and high $\bar{V}_{SG}$ values where respectively, stratified and droplet flow occurred. The magnitude of the hold-up and the slopes of the lines increased steadily with increasing $\bar{V}_{SL}$. Data by Spedding and Nguyen [10] obtained for 0.0454 m (i.d.) pipe are included and showed similar trend with the exception that the position and slope of the lines were slightly greater (under corresponding conditions) for the smaller diameter. The limited data of Beggs and Brill [2] also gave general agreement with these findings.

Figures 8 and 9 give results for inclined flow under corresponding conditions to those used in Fig. 7. For the purposes of discussion, Fig. 10 groups the data for all three angles for the highest $\bar{V}_{SL}$ value of 4.11×10^{-2} m s^{-1}. Excluding low liquid flows, in general $\alpha = +5^\circ$ data possessed a greater value of $\bar{R}_L$ for corresponding flow conditions. At low $\bar{V}_{SG}$ values the slug flow regime was formed for $\alpha = +5^\circ$ in contrast to the stratified regime for the corresponding horizontal and $\alpha = -5^\circ$ conditions. It was not unexpected therefore, that the $\bar{R}_L$ for $\alpha = +5^\circ$ angle would be greater since, in general, liquid hold-up for stratified flow would be less than for the slug regime. As the gas rate was increased the hold-up tended to converge and run along a parallel path as similar flow regimes were developed. At no point did the $\alpha = +5^\circ$ data fall below that of the $\alpha = 0^\circ$ data even for the azympotic region at higher $\bar{V}_{SG}$ rates.

Downward $\alpha = -5^\circ$ data possessed lower liquid hold-up values that the corresponding condition at other angles for $\bar{V}_{SG} < 20$ m s^{-1}. The profile of the $\alpha = -5^\circ$ data in this region was flat since the stratified plus inertial wave regime was present. At some point ($\bar{V}_{SG}$ between 1 and 20 m s^{-1} rising with $\bar{V}_{SL}$ value) the $\alpha = -5^\circ$ data crossed over the $\alpha = 0^\circ$ plot. If $\bar{V}_{SL} < 0.03$ m s^{-1} the $\alpha = -5^\circ$ data subsequently went on to cross the $\alpha = +5^\circ$ data and then run parallel to it thereafter. For $\bar{V}_{SL} \geqslant 0.03$ m s^{-1} the $\alpha = 0^\circ$ data were crossed alone.

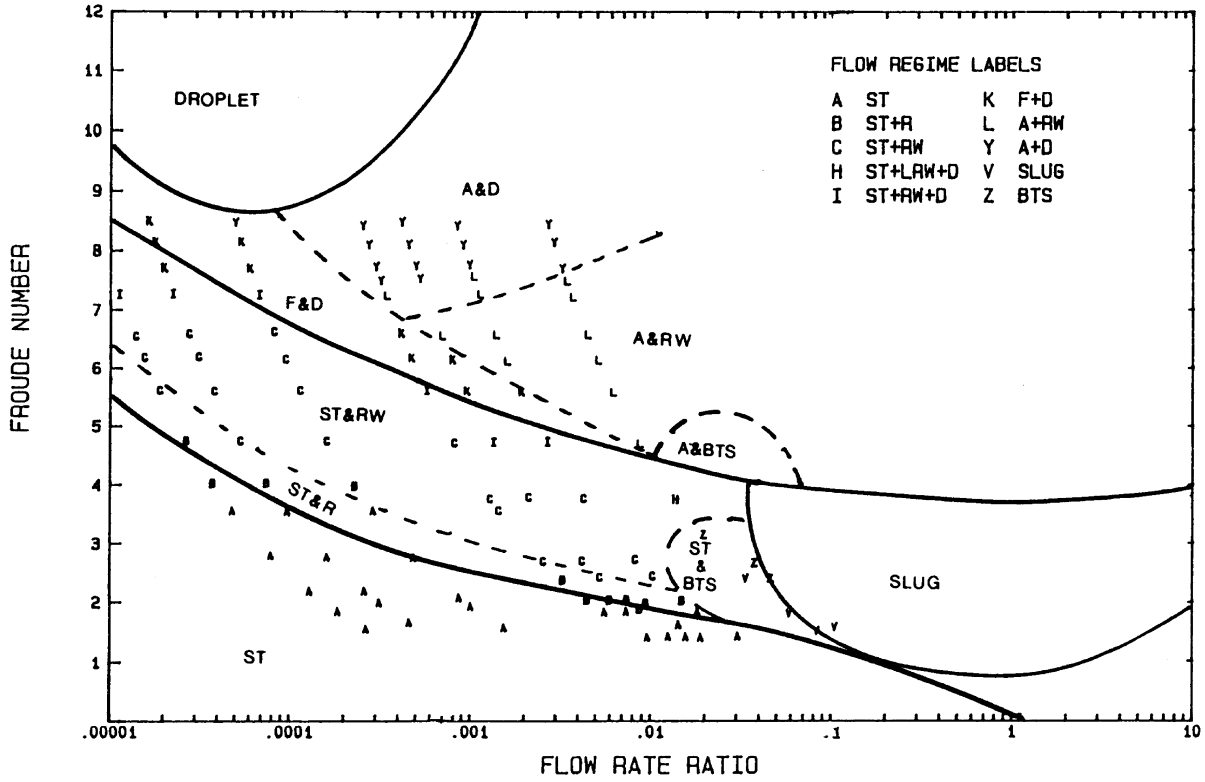

Fig. 3. The modified Spedding and Nguyen [5] map compared to the horizontal air–water data for 0.0508 m (i.d.) pipe.

Thus at $\bar{V}_{SG} = 10\,m\,s^{-1}$ the hold-up values rose steadily as the angle went from $\alpha = -5^\circ$ through $\alpha = 0^\circ$ to $\alpha = +5^\circ$. For $\bar{V}_{SG} > 10\ ms^{-1}$ initially the $\alpha = +5^\circ$ data were higher than and paralleled the corresponding $\alpha = 0^\circ$ data. However the $\alpha = -5^\circ$ data became larger in value than either the $\alpha = +5^\circ$ or $\alpha = 0^\circ$ data except when $\bar{V}_{SL} > 0.03\ m\,s^{-1}$.

From a practical stand point if operation was below $\bar{V}_T < 1\ m\,s^{-1}$ (which it would be in many oil/gas installations in order to handle static electricity problems) the liquid hold-up will be lowest in downward flow and highest in upward flow. However, if $\bar{V}_T > 20\ m\,s^{-1}$ the liquid hold-up will be lowest in horizontal flow and highest in upward flow except when $\bar{V}_{SL} > 0.03\ m\,s^{-1}$ where upward flow would have the highest hold-up value.

Numerous models have been developed for the prediction of hold-up in two-phase flow for various geometric conditions of conduit diameter and inclination. In many cases the individual models were reported to give good agreement with data used for the model development. However, often the models did not perform satisfactorily when checked against independently obtained and validated data.

The usual way of ascertaining the performance of a model is to compare the average error and standard deviation of the predicted value against the data. However, Spedding et al. [22, 23] have shown the use of standard deviation to be inappropriate. More sophisticated statistics gave the same result as a well chosen spread of both the errors and the average value.

Spedding et al. [24–28] have detailed models that were successful in predicting hold-up within an average of $\pm 13\%$ and a $\pm 30\%$ spread for horizontal [24–26] and slightly inclined pipes [27, 28]. Checks using data from this work and elsewhere [2, 10, 11] have been carried out and the results showed general agreement with the predictions found by Spedding et al. [24–28]. A summary is given in Table 1. There were other models, not shown in Table 1, that were successful in predicting some flow regimes but not over the range of angles. These models were excluded from the recommendation of Table 1. The results showed an increase in prediction performance with increasing pipe diameter. In general downward flow proved to be easiest to predict and upward flow was the most difficult. Since multi-phase transport is an uncertain theoretical area at this stage of development any pre-

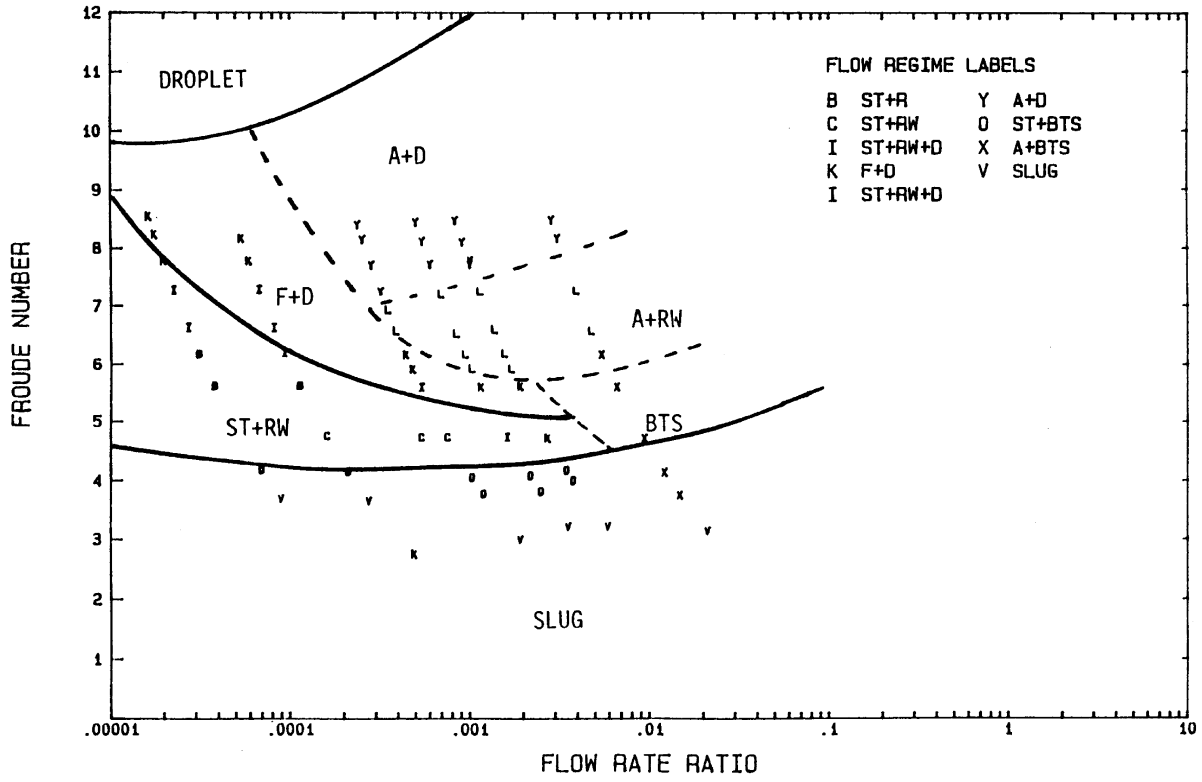

Fig. 4. The modified Spedding and Nguyen [5] map compared to the air–water data for 0.0508 m (i.d.) pipe at $\theta = +5^{\circ}$.

diction should not depend on the result from just one model but be subject to confirmation by the result of a number of different models in order to obtain a reliable result. For this reason a number of models are suggested for each flow regime and angle of inclination.

Equation (1) gives a new relation between hold-up, Q_L/Q_T and pipe diameter using the condition, suggested by Spedding and Hand [44, 45], that $\bar{V}_{SG} > 6$ m s^{-1}.

$$\bar{R}_L = (3.5+d)\left(\frac{Q_L}{Q_T}\right)^{0.7} \quad (1)$$

The model was within $\pm 30\%$ of data for horizontal air–water data at three different pipe diameters. Figure 11 illustrates the result for the data of this work. It should be noted that equation (1) will not predict the smooth stratified, stratified inertia wave, stratified blown-through-slug, bubble, slug and plug regime. In addition the data showed a minor effect of liquid rate which is handled by equations (2) and (3).

$$\frac{\bar{R}_G}{R_L} = ([2.183d+0.041]\bar{V}_{SL}^{-0.79})\left(\frac{Q_G}{Q_L}\right)^{0.04} - (1-H(\bar{V}_{SL}-0.01035))\left(\frac{0.024}{\bar{V}_{SL}}-2.3170\right) \quad (2)$$

where the Heaviside function

$$H(\bar{V}_{SL}-0.01035) = \frac{1}{2}\left(1+\frac{2}{\pi}\int_0^{\infty}\frac{\sin(\bar{V}_{SL}-0.01035)}{u}\,du\right) \quad (3)$$

When the data were used to check these more complex relations the spread was reduced considerably to approximately half of the value shown in Fig. 11. Thus equations (1)–(3) used in conjunction with the Nicklin et al. [41] model for intermittent flow and the Spedding–Hand [31] and Lockhart–Martinelli [37] models, can predict the whole range of flow regimes.

A development for prediction hold-up by Spedding and Hand [44, 45] will be handled later in the next section.

2.3. Pressure drop

In general the pressure drop data for horizontal and inclined flows presented as a series of curves with the same general form but with increasing total pressure loss as the liquid rate increased. For horizontal flow a series of parallel straight lines were formed on a log–log plot as shown in Fig. 12. At low gas rates, where stratified flow occurred, the pressure drop fell away towards the open channel condition. At high gas rates the pressure drop altered slope and rose above the straight line condition

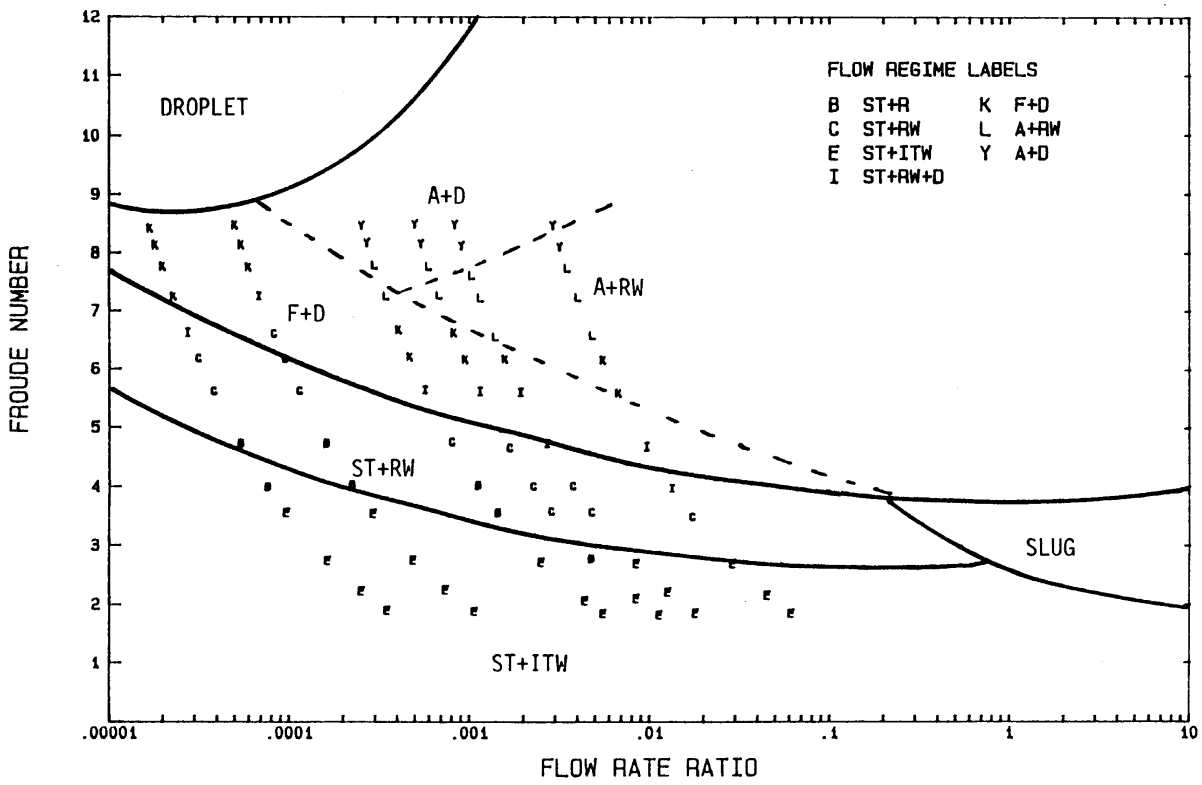

Fig. 5. The modified Spedding and Nguyen [5] map compared to the air–water data for 0.0508 m (i.d.) pipe at $\theta = -5°$.

at the point where the flow regime changed from annular roll wave to annular droplet flow. The increase in pressure drop experienced at this point was caused by the extra energy needed from the gas to form liquid droplets. The pressure drop data for $\alpha = +5°$, shown in Fig. 13, were much more complex. For the lowest liquid flow, the average total pressure drop was high at low gas rates since the flow was in the slug regime. The pressure loss fell with increasing gas rate until at about $\bar{V}_{SG} \approx 10$ m s^{-1} the average pressure drop became negative at the onset of the blow-through-slug regime. Kokal and Stanislav [8] also reported low pressure gradients over a wide range of flows due to the formation of such phenomena as stratification, phase discontinuities and other complex mechanisms. As the gas rate was further increased the pressure drop also increased and formed a straight line region that was very similar to that obtained with horizontal flow but over a decreased range of gas flows. In this high gas flow region about $\bar{V}_{SG} = 50$ m s^{-1} the pressure loss was largely unaffected by the angle of inclination. Thus the general trend with increasing gas rate was an initial high value of pressure loss followed by a steep fall to a minimum and then a rise to the straight line region similar to horizontal flow. As the liquid rate was increased the negative pressure loss region decreased and eventually disappeared and gave a positive minimum at about $\bar{V}_{SG} = 10$ m s^{-1} in the blow through slug regime. This would be a preferred operational region for $\alpha = +5°$ flow.

Figure 14 sets out the pressure drop data for the $\alpha = -5°$ geometry. At low gas rates in the stratified type regime the pressure drop changed very little with increased gas flow. Above $\bar{V}_{SG} = 10$ m s^{-1} the data formed into an approximate straight line region not unlike that observed for horizontal flow. Figure 15 presents data for all three angles at the highest liquid velocity $\bar{V}_{SL} = 0.0411$ m s^{-1}. The inter-relationships between the data were complex with a number of cross-over points occurring. For gas flows of $\bar{V}_{SG} \leqslant 10$ m s^{-1} the horizontal condition gave the lowest pressure drop. For $\bar{V}_{SG} = 10$–45 m s^{-1} the $\alpha = +5°$ data gave the least pressure drop and the horizontal geometry the largest. Above $\bar{V}_{SG} = 45$ m s^{-1} the $\alpha = -5°$ geometry gave the greatest pressure drop and the $\alpha = +5°$ the least. The frictional pressure drop data are also detailed on Fig. 15 and indicate that for low gas flow rates $\bar{V}_{SG} < 5$ m s^{-1} a negative frictional loss was achieved for upward flows. With downward flows for the same condition $\bar{V}_{SG} < 5$ m s^{-1} the frictional pressure drop was negligible and the flat portion of the total pressure drop curve was entirely due to the head of

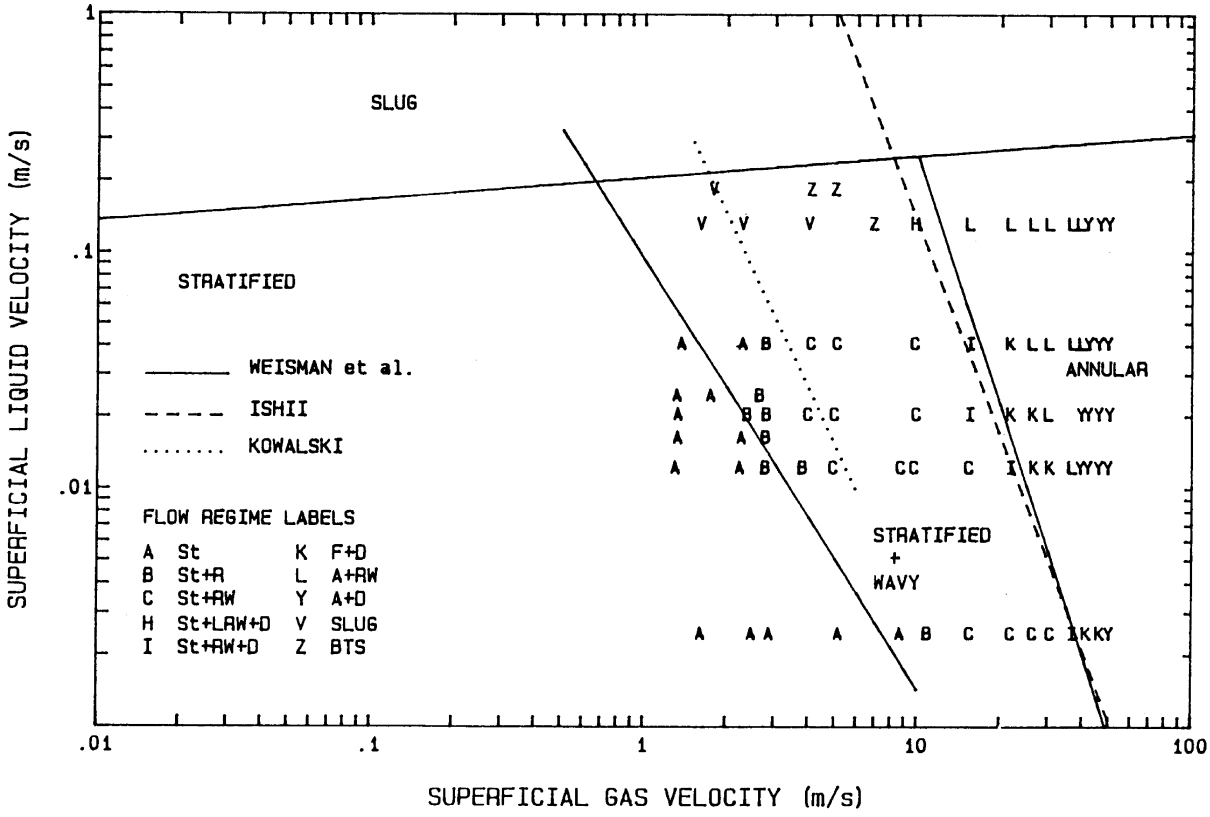

Fig. 6. The Weisman et al. [15] transition criteria compared to the horizontal air–water data for 0.0508 m (i.d.) pipe.

fluid present in the tube. The effect of head on the total pressure drop was only a few percent at high gas rates. Data from Spedding and Nguyen [10] are also plotted on Figures 12–14 and indicate general agreement with the current work. This stands in contrast to the data of Beggs and Brill [2] etc. [8, 46, 47] which exhibited considerable variation from the present work.

The pressure loss fluctuations for horizontal flow were significantly different to that for the uphill slug flow pattern. The characteristic steep front, body and tail of the horizontal slug pressure profile were absent in the $\alpha = +5^\circ$ data. In addition, both the amplitude and frequency of the pressure peaks were much greater. After each peak caused by the passing slug the pressure loss dropped well below the zero line. This was caused by the liquid falling back down the pipe after each slug had passed.

The smooth pressure loss fluctuations normally associated with horizontal stratified flow did not exist in downhill flow. In general for the downhill mode the range of pressure drop variation was greater and there were more fluctuations in the profile. This was in addition to a significant expansion in the range of flow rates over which the stratified regime occurred.

Kokal and Stanislav [8] reported that for air–oil downward flow the liquid on the base of the pipe moved faster than for the corresponding horizontal condition due to the effect of gravity and resulted in lower liquid hold-up for these flows. In uphill flow the effect was reversed. They considered downhill stratified flow to be a complex flow situation since stratification and secondary flow patterns were set-up in the liquid phase. Mukherjee and Brill [3] agreed with these general observations on inclined flow.

These differences in the characteristic pattern of pressure drop between the three different angles for the same flow regime highlight the problems which have been encountered when attempting to predict performance. Ferguson and Spedding [48] have shown that the models of Olujic [49] and Spedding and Hand [44] predicted pressure drop for certain flow regimes within an average of $\pm 15\%$ and a $\pm 30\%$ spread for both horizontal [44, 48] and downward inclined flows [22]. Figures 16 and 17 show the two models to be useful in prediction of pressure

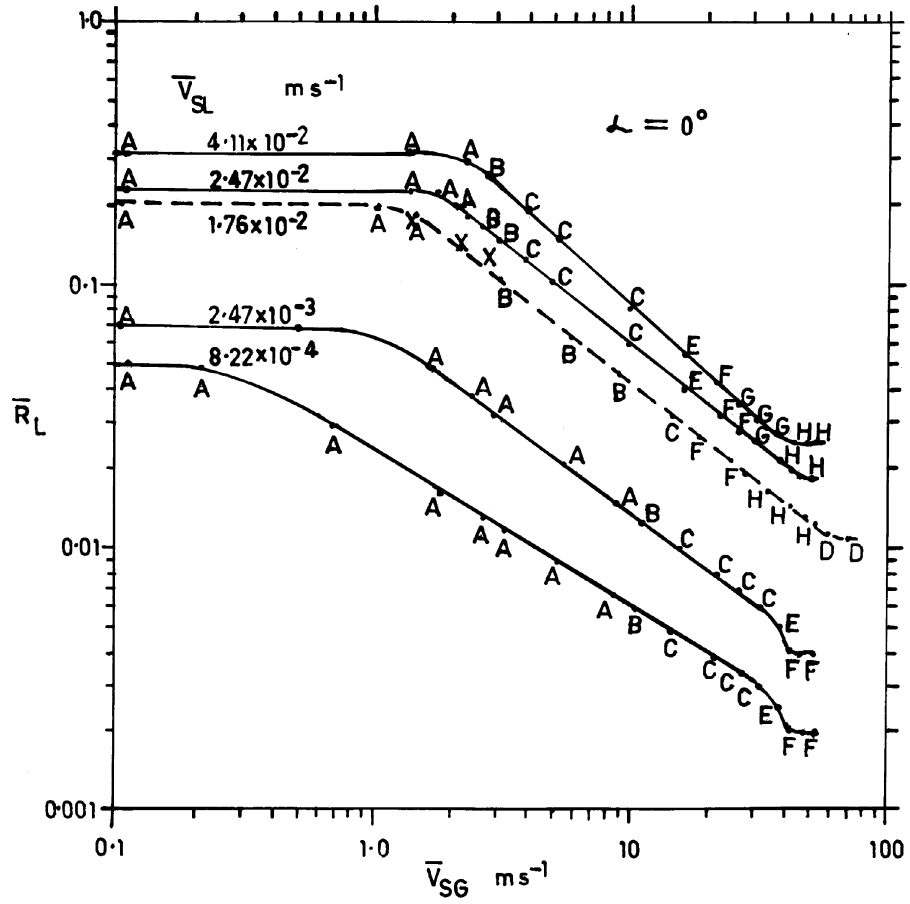

Fig. 7. Liquid hold-up $\bar{R}_L$ against superficial gas velocity $\bar{V}_{SG}$ for $\alpha = 0°$ with co-current air–water flow. —— 0.0508 m (i.d.) ... 0.0454 m (i.d.), Spedding and Nguyen [10]. xxx 0.0254 m *d*., $\bar{V}_{SL} = 1.645 \times 10^{-2}$ m s^{-1} Beggs and Brill [2]. Flow regimes: A = St; B = St+R; C = St+RW; D = D; E = St+RW+D; F = F+D; G = A+RW; H = A+D.

drop for horizontal flow and in the case of the Spedding and Hand [44] model for hold-up as well. Prediction for the inclined data as shown in Figs 18–21 was acceptable (but not as good as in the horizontal mode) for pressure drop but not for hold-up.

3. Conclusions

Data are reported for flow regimes, holdup and pressure drop in a 0.0508 m (i.d.) pipe at angles of +5, 0 and −5°.

All existing flow regime maps failed in some manner to correctly predict data. The Spedding and Nguyen [5] map gave good prediction of the slug to stratified regimes for all diameters. This was consistent with the use of *Fr* as a mapping parameter since it correctly modelled mixing in turbulent liquid systems. Transition criteria by Kowalski [21] for stratified ripple to roll wave, Kokal and Stanislov [8] for slug to blow-through-slug and Ishii and Grolmes [19, 20] for stratified to film plus droplet all proved to be reliable.

Corrected maps were proposed for prediction for horizontal and slightly inclined flows that will, with the proven transition criteria give reasonable prediction.

At high gas flow rates both hold-up and pressure drop was the same for all inclinations, due to the formation of annular type flow which effectively negated any influence of gravity. For other flow conditions the effect of inclination on two-phase parameters was complex.

Upward flow generally possessed the highest liquid hold-up due to the tendency to form slug flow. Downward flow gave the lowest hold-up at low gas rates while horizontal flow gave the lowest value at higher gas rates.

Pressure drop was different either side of a superficial gas velocity of about 10 m s^{-1}. Below this value upward flow possessed the highest pressure loss and the horizontal flow the lowest. Above $\bar{V}_{SG} = 10$ m s^{-1} the

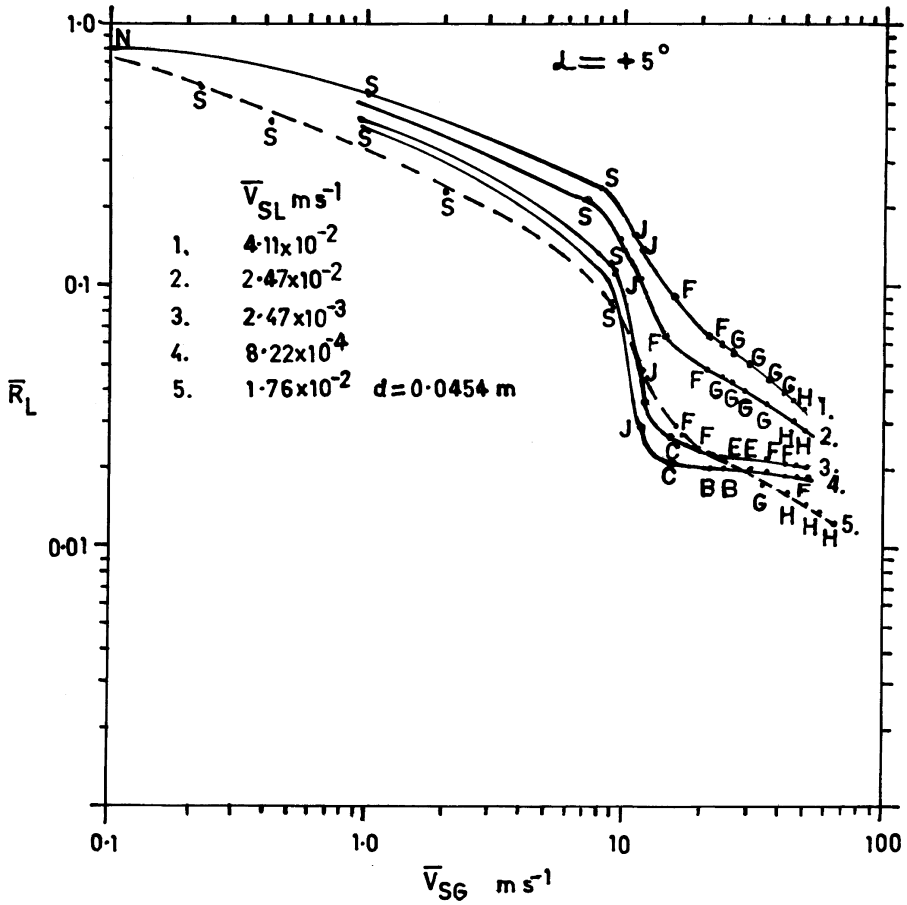

Fig. 8. Liquid hold-up $\bar{R}_L$ against superficial gas velocity $\bar{V}_{SG}$ for $\alpha - +5°$ with co-current air–water flow. —— 0.0508 m (i.d.) ... 0.0454 m (i.d.), $\alpha = +2.75°$, Spedding and Nguyen [10]. Flow regimes: B = St+R; C = St+RW; F = F+D; G = A+RW; H = A+D, J = St+BTS; S = S1; N = B.

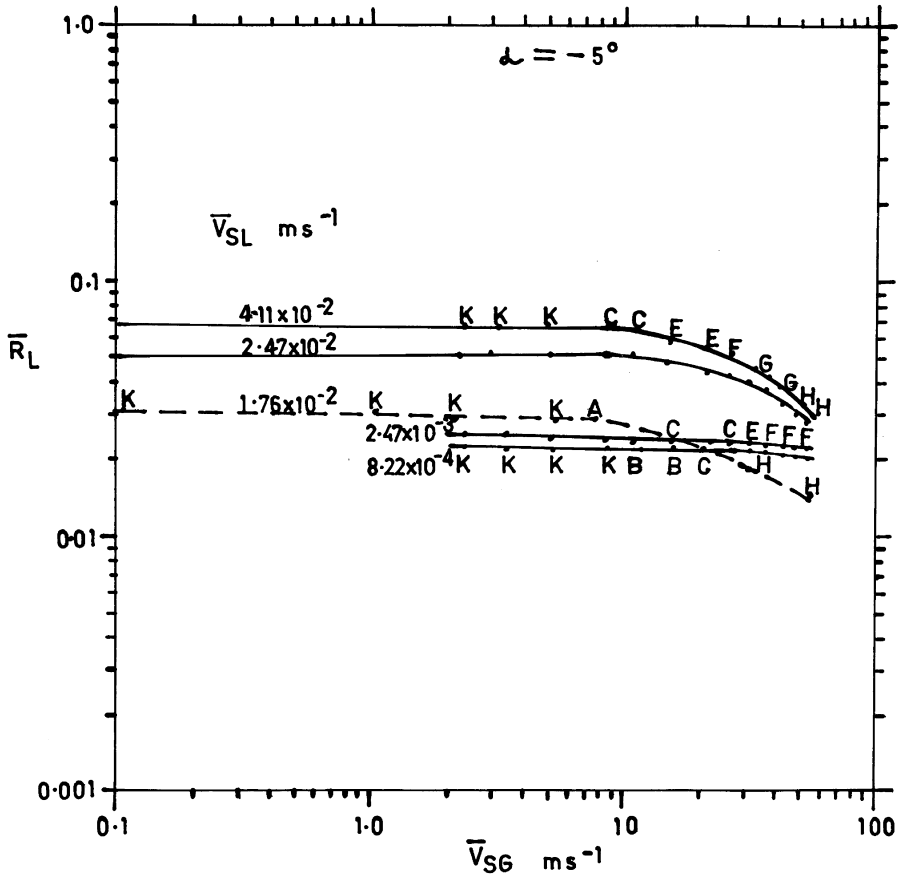

Fig. 9. Liquid hold-up $\bar{R}_L$ against superficial gas velocity $\bar{V}_{SG}$ for $\alpha = -5°$ with co-current air–water flow. —— 0.0508 m (i.d.) ... 0.0454 m (i.d.), $\alpha = -6.17°$, Spedding and Nguyen [10]. Flow regimes: B = St+R; C = St+RW; E = St+RW+D; F = F+D; G = A+RW; H = A+D, K = St+IW.

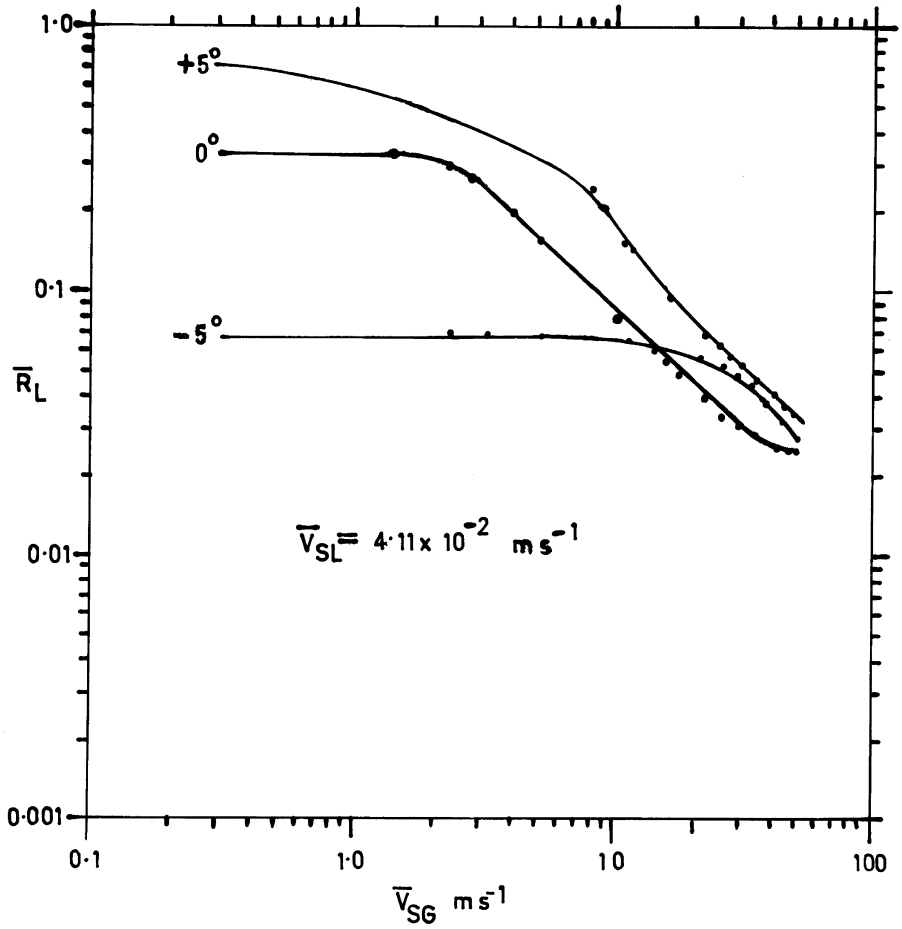

Fig. 10. The effect of pipe angle on the liquid hold-up $\bar{R}_L$ against superficial gas velocity $\bar{V}_{SG}$.

Table 1
Models successfully predicting hold-up for various flow regimes and diameters 0.0260–0.0935 m

Regime	0°		−5° and +2.75°		+5° and +6.17°	
St	Kawaji	[30]	N/A		Kawaji	[30]
	Spedding–Hand	[31]			Spedding–Hand	[31]
	Hart	[29]			Taitel–Dukler	[32]
					Chisholm–Armand	[33]
					Chisholm–Laird	[34]
St + R	Hart	[29]	Hart	[29]	Hart	[29]
	Kawaji	[30]	Kawaji	[30]	Spedding–Spence	[25]
	Spedding–Hand	[31]	Spedding–Hand	[31]	Taitel–Dukler	[32]
			Taitel–Dukler	[32]	Chisholm–Laird	[34]
			Chisholm–Armand	[33]	Spedding–Chen S	[39]
			Nishino	[36]		
St + RW	Kawaji	[30]	Kawaji	[30]	Kawaji	[30]
	Spedding–Hand	[31]	Spedding–Hand	[31]	Spedding–Hand	[31]
	Lockhart–Martinelli	[37]	Lockhart–Martinelli	[37]	Lockhart–Martinelli	[37]
	Hart	[29]	Taitel–Dukler	[32]	Taitel–Dukler	[32]
	Turner–Wallis	[40]	Hart	[29]	Chisholm–Laird	[34]
			Turner–Wallis	[40]	Spedding–Chen S	[39]
			Spedding–Chen II	[39]	Chen	[35]
			Hughmark	[38]	Nicklin	[41]
St + 1W	Kawaji	[30]	N/A		Kawaji	[30]
	Spedding–Hand	[31]			Spedding–Hand	[31]
	Lockhart–Martinelli	[37]			Taitel–Dukler	[32]
	Chisholm–Armand	[33]				
	Chisholm–Laird	[34]				
	Chen	[35]				
B	Nicklin	[41]	Nicklin	[41]	Nicklin	[41]
	Bonnecaze	[42]	Bonnecaze	[42]	Bonnecaze	[42]
	Rouhani II	[43]	Rouhani II	[43]	Rouhani II	[43]
	Hughmark	[38]			Chisholm–Laird	[34]
	Nishino	[36]			Chen	[35]
S	Nicklin	[41]	Nicklin	[41]	Nicklin	[41]
	Bonnecaze	[42]	Bonnecaze	[42]	Bonnecaze	[42]
					Spedding–Spence	[25]
					Chisholm–Laird	[34]
					Chen	[35]
					Nishino	[36]
					Spedding–Chen S	[39]
St + BTS	Lockhart–Martinelli	[37]	Lockhart–Martinelli	[37]	Lockhart–Martinelli	[37]
	Hughmark	[38]	Hughmark	[38]	Hughmark	[38]
	Turner–Wallis	[40]	Turner–Wallis	[40]	Turner–Wallis	[40]
	Hart	[29]	Hart	[29]	Spedding–Chen II	[27]
	Kawaji	[30]	Kawaji	[30]	Chisholm–Laird	[34]
	Spedding–Hand	[31]	Spedding–Hand	[31]	Chen	[35]
	Nicklin	[41]	Spedding–Chen II	[39]	Nishino	[36]
			Rouhani I, II	[43]	Nicklin	[41]
					Rouhani I, II	[43]

(*continued on next page*)

Table 1—*continued*

Regime	0°		−5° and +2.75°		+5° and +6.17°	
A+BTS	Spedding–Spence	[25]	Spedding–Spence	[25]	Spedding–Spence	[25]
	Chen	[35]	Chen	[35]	Chen	[35]
	Nishino	[36]	Nishino	[36]	Nishino	[36]
	Lockhart–Martinelli	[37]	Lockhart–Martinelli	[37]	Lockhart–Martinelli	[37]
	Spedding–Chen S II	[39]	Spedding–Chen S II	[39]	Spedding–Chen S II	[39]
	Hart	[29]	Hart	[29]	Chisholm–Laird	[34]
					Turner–Wallis	[40]
F+D	Kawaji	[30]	Kawaji	[30]	Kawaji	[30]
	Spedding–Hand	[31]	Spedding–Hand	[31]	Spedding–Hand	[31]
	Hart	[29]	Nishino	[36]	Spedding–Spence	[25]
	Taitel–Dukler	[32]	Spedding–Chen S II	[39]	Hart	[29]
	Chisholm–Armand	[33]			Taitel–Dukler	[32]
	Lockhart–Martinelli	[37]			Chisholm–Armand	[33]
					Chisholm–Laird	[34]
					Chen	[35]
					Nishino	[36]
					Lockhart–Martinelli	[37]
					Spedding–Chen S	[39]
A+W	Spedding–Spence	[25]	Spedding–Spence	[25]	Spedding–Spence	[25]
	Hart	[29]	Hart	[29]	Hart	[29]
	Spedding–Hand	[31]	Spedding–Hand	[31]	Spedding–Hand	[31]
	Chisholm–Armand	[33]	Chisholm–Armand	[33]	Chisholm–Armand	[33]
	Chen	[35]	Chen	[35]	Chen	[35]
	Nishino	[36]	Nishino	[36]	Nishino	[36]
	Spedding–Chen S II	[39]	Spedding–Chen S II	[39]	Spedding–Chen S II	[39]
	Chisholm–Laird	[34]	Lockhart–Martinelli	[37]	Chisholm–Laird	[34]
	Lockhart–Martinelli	[37]	Hughmark	[38]	Hughmark	[38]
A+D	Spedding–Spence	[25]	Spedding–Spence	[25]	Spedding–Spence	[25]
	Hart	[29]	Hart	[29]	Hart	[29]
	Chen	[35]	Chen	[35]	Chen	[35]
	Spedding–Chen S II	[39]	Spedding–Chen S II	[39]	Spedding–Chen S II	[39]
					Spedding–Hand	[31]
					Lockhart–Martinelli	[37]
					Turner–Wallis	[40]
D	Spedding–Hand	[31]	Spedding–Hand	[31]	Spedding–Hand	[31]
	Taitel–Dukler	[32]	Taitel–Dukler	[32]	Taitel–Dukler	[32]
					Chisholm–Armand	[33]
					Chen	[35]
					Nishino	[36]
					Turner–Wallis	[40]
A+S	Nicklin	[41]	Nicklin	[41]	Nicklin	[41]
B+S					Chisholm–Armand	[33]
					Chisholm–Laird	[34]
					Chen	[35]

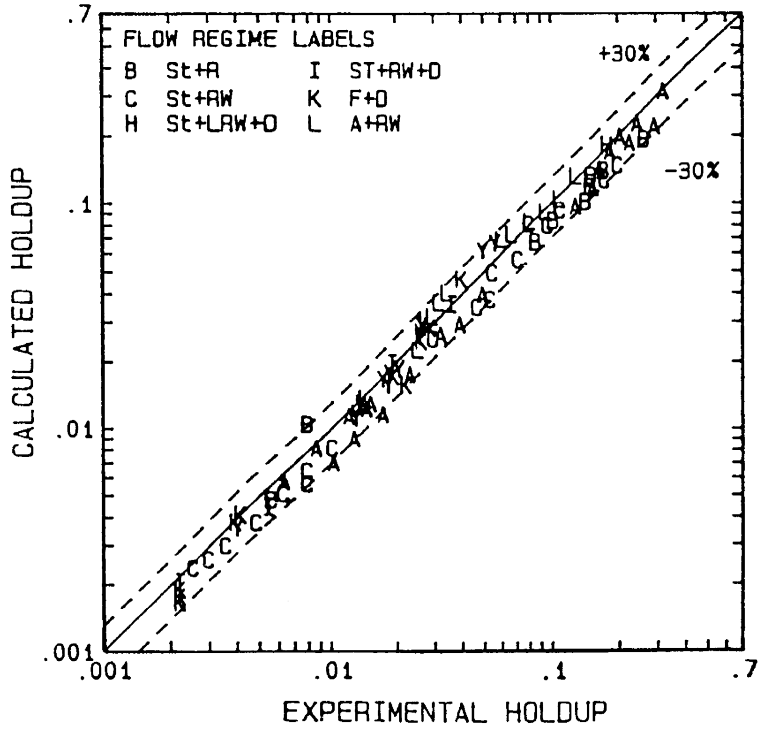

Fig. 11. Comparison between hold-up calculated using the Ferguson–Spedding relation of equation (1) compared to experimental values from this work for $\alpha = 0^{\circ}$.

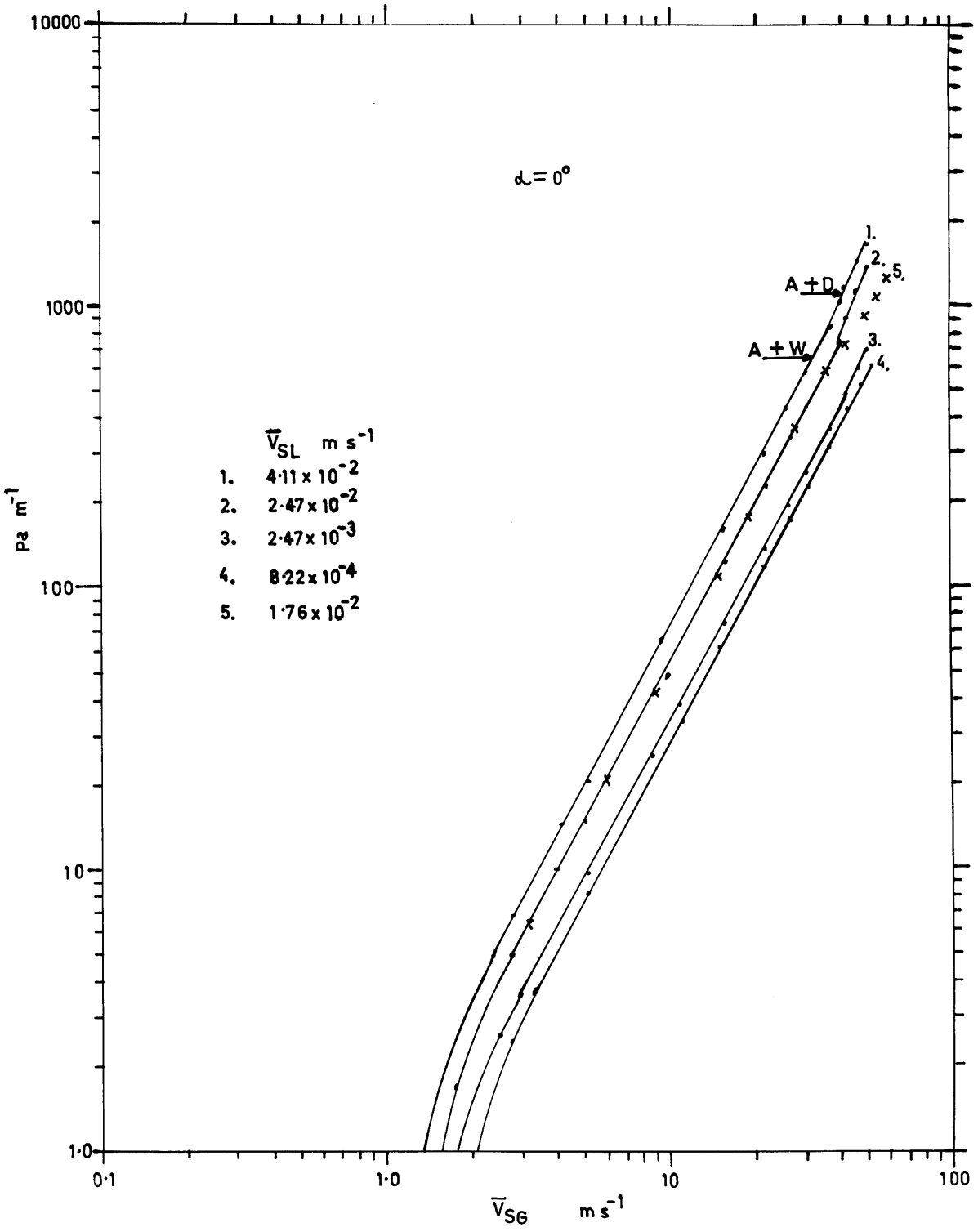

Fig. 12. Total pressure loss against superficial gas velocity $\bar{V}_{SG}$ for $\alpha = 0^{\circ}$ with co-current air–water flow. x 0.0454 m (i.d.), Spedding and Nguyen [10].

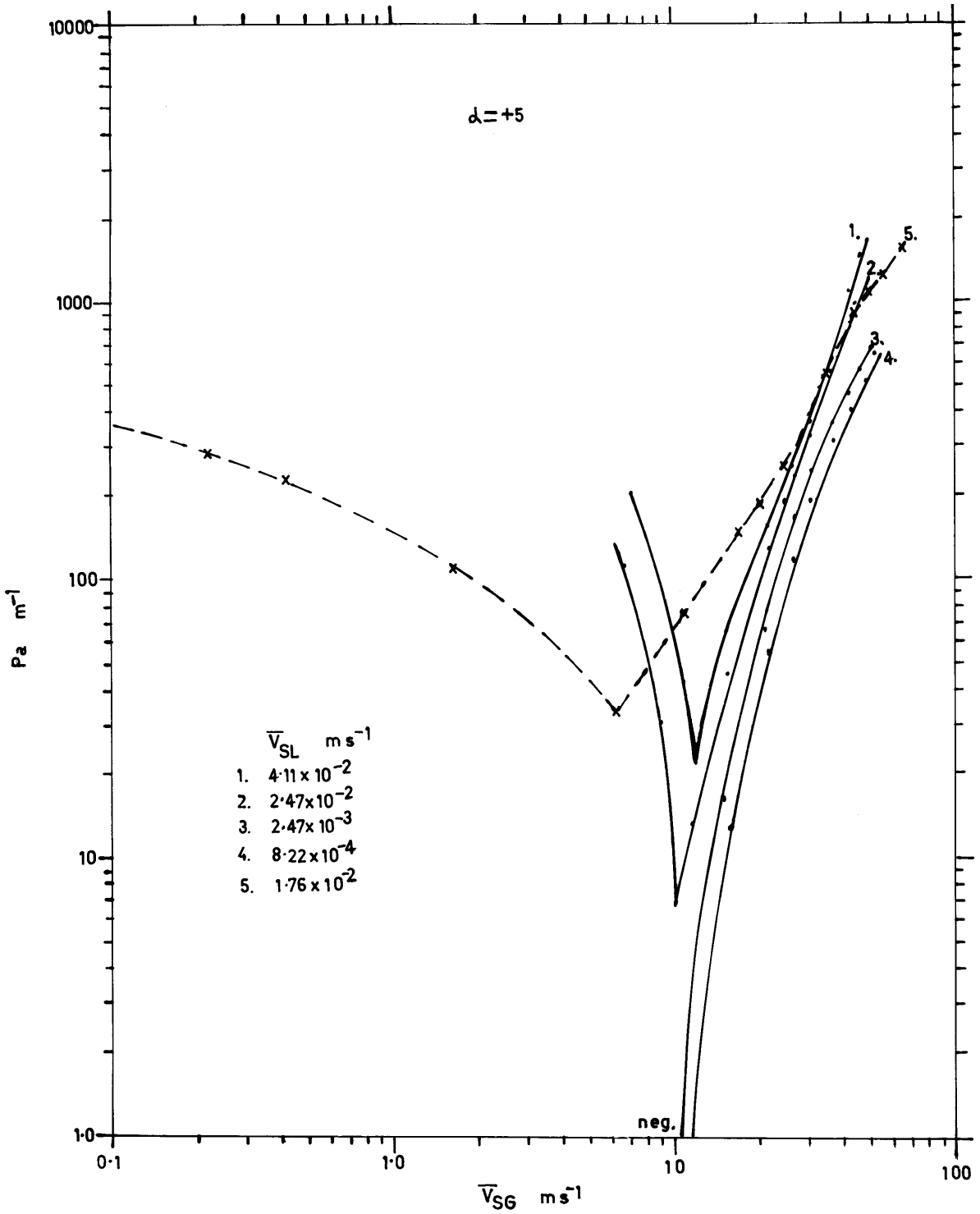

Fig. 13. Total pressure loss against superficial gas velocity $\overline{V}_{SG}$ for $\alpha = 5^\circ$ with co-current air–water flow. x–x 0.0454 m (i.d.), $\alpha = +2.75^\circ$, Spedding and Nguyen [10].

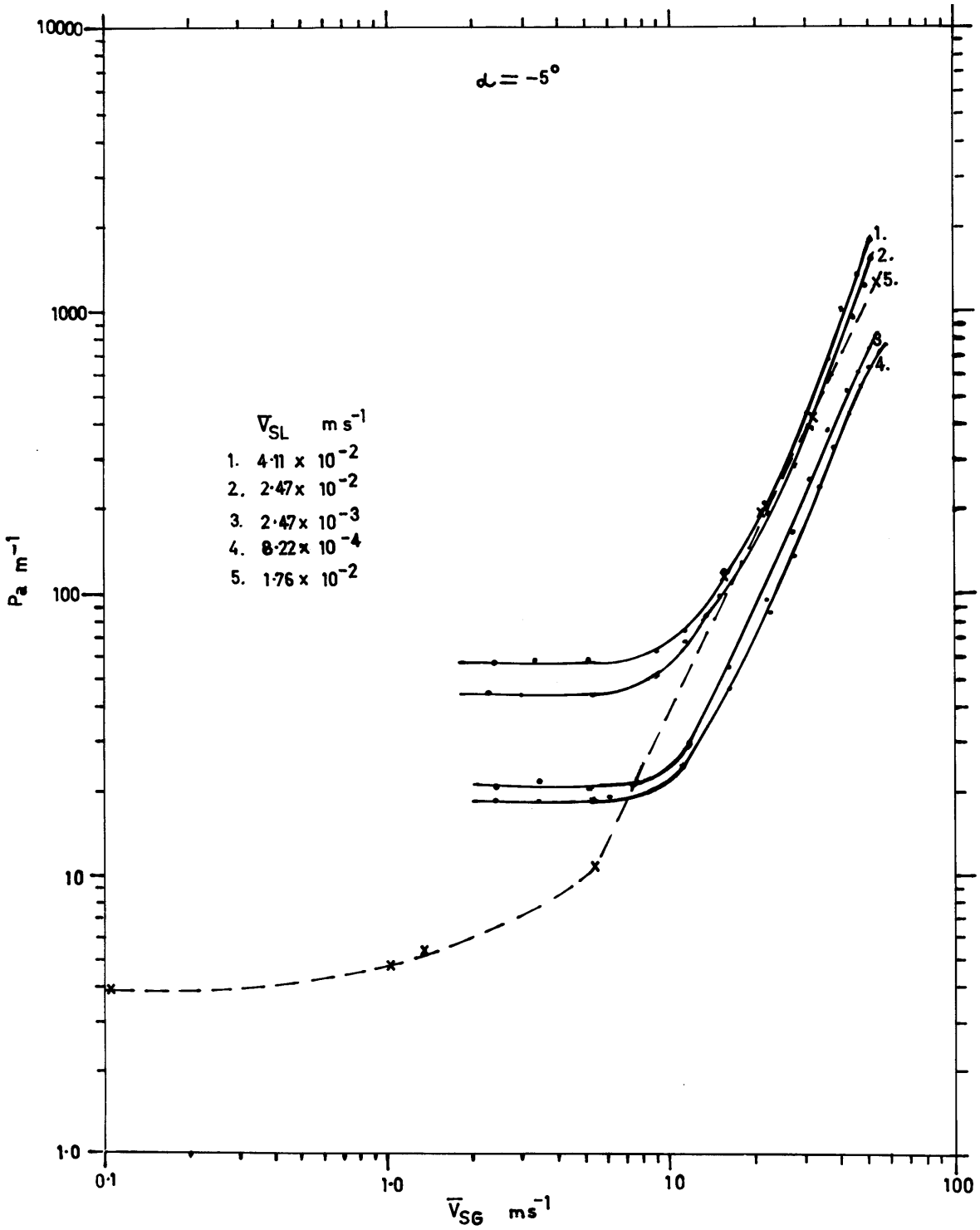

Fig. 14. Total pressure loss against superficial gas velocity $\bar{V}_{SG}$ for $\alpha = -5^\circ$ with co-current air–water flow. x–x 0.0454 m (i.d.), $\alpha = +6.17^\circ$, Spedding and Nguyen [10].

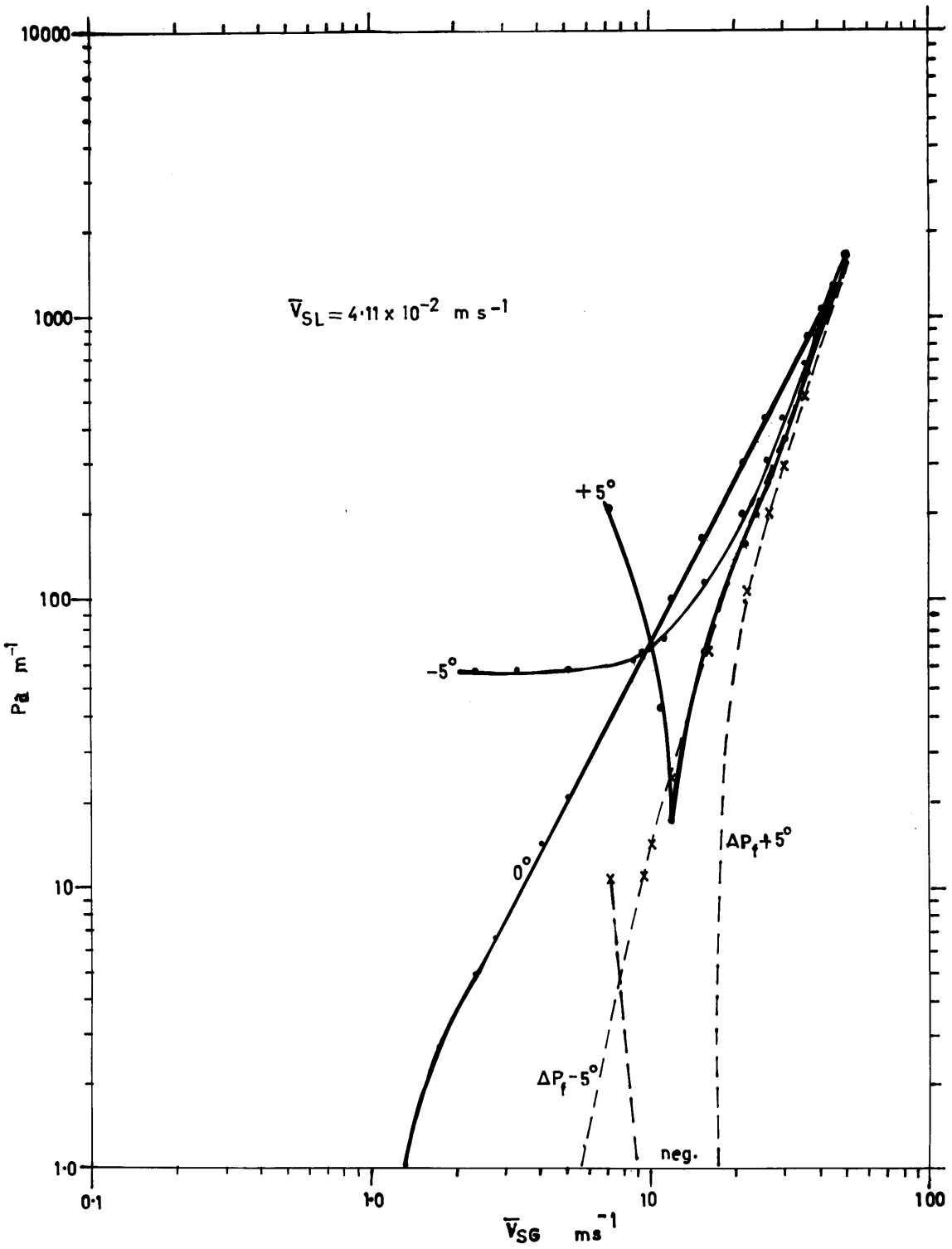

Fig. 15. The effect of pipe angle on the total pressure loss (——) and frictional pressure loss (x–x) against superficial gas velocity $\bar{V}_{SG}$.

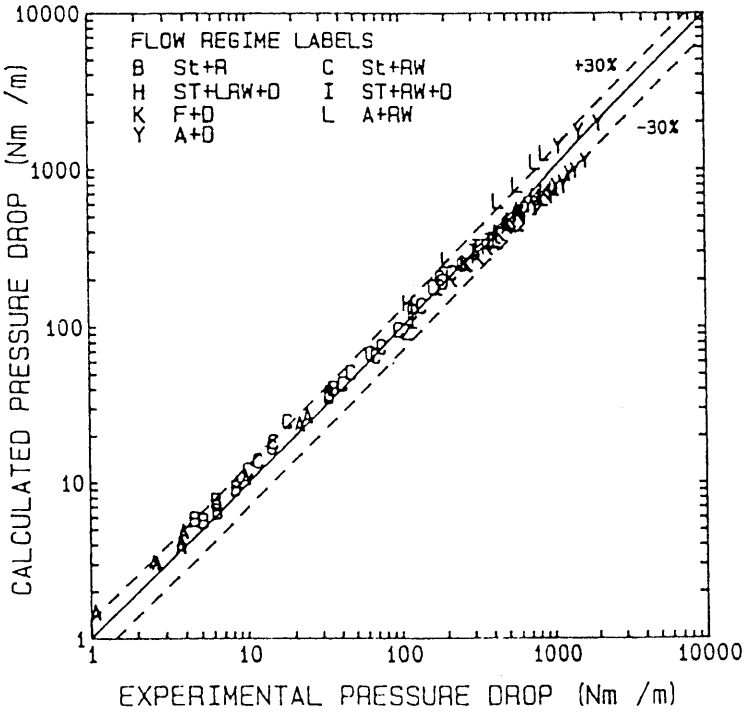

Fig. 16. Comparison between calculated pressure loss by the Olujic [49] method and data of this work, $d=0$.

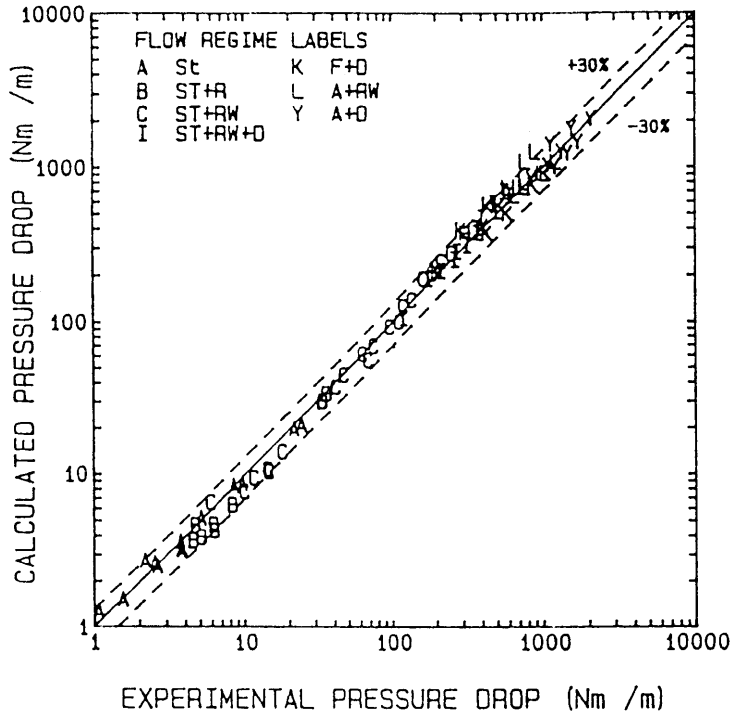

Fig. 17. Comparison between the calculated pressure loss using the Spedding–Hand [44] method and experimental data from this work, $\alpha = 0$.

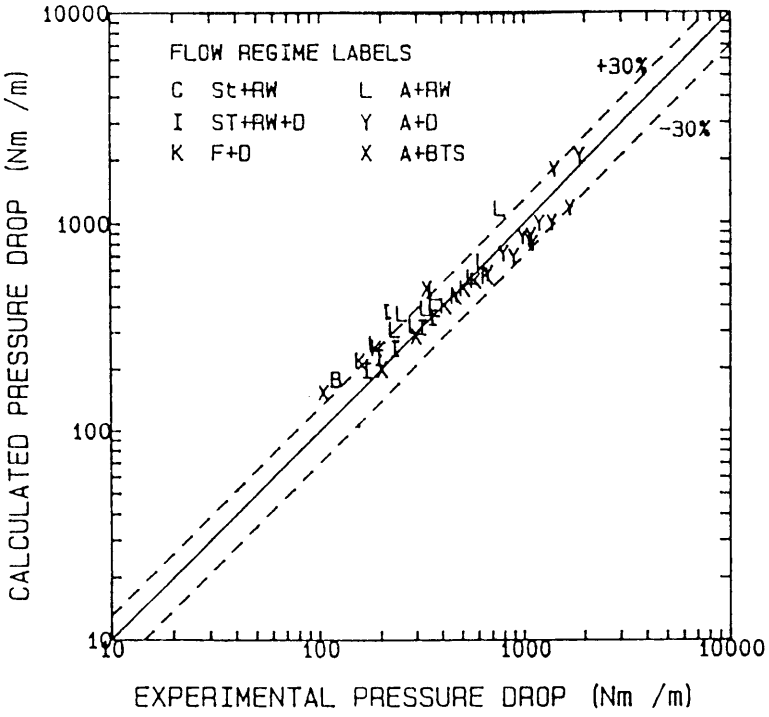

Fig. 18. Comparison between the calculated pressure drop using the Olujic [49] method and experimental data from this work for $\alpha = +5$.

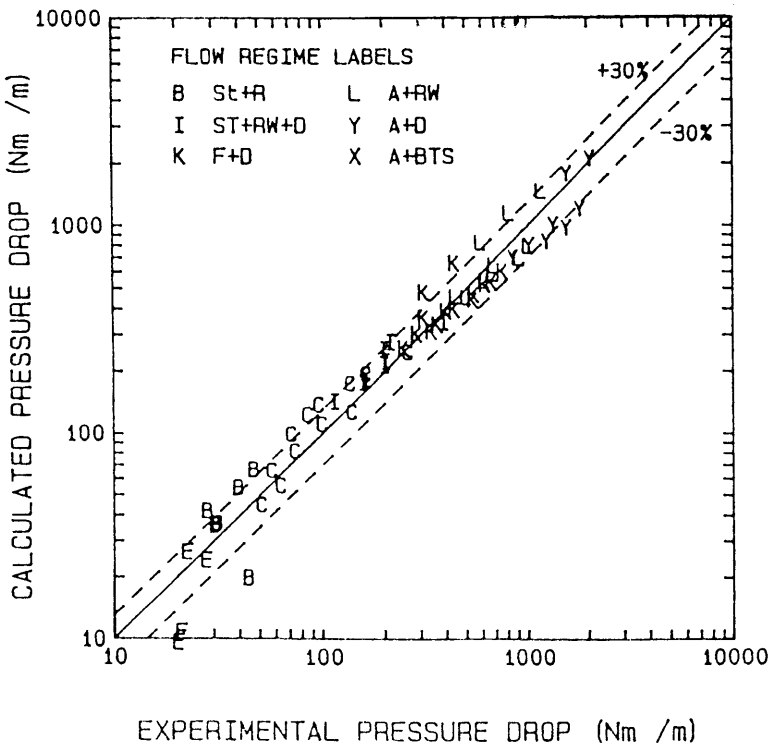

Fig. 19. Comparison between the calculated pressure drop using the Olujic [49] method and experimental data from this work for $\alpha = -5$.

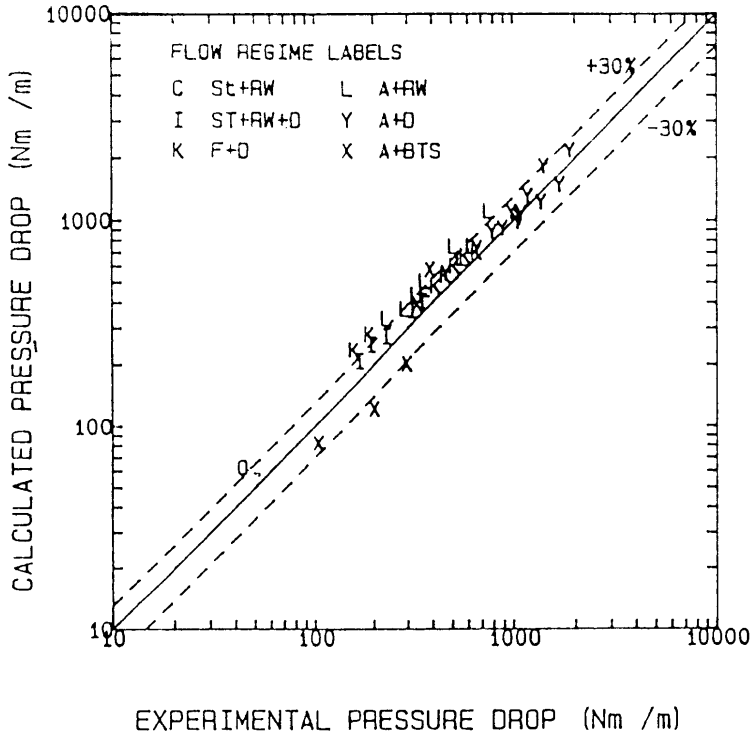

Fig. 20. Comparison between the calculated pressure drop using the Spedding–Hand [44, 45] method and experimental data from this work for $\alpha = +5$.

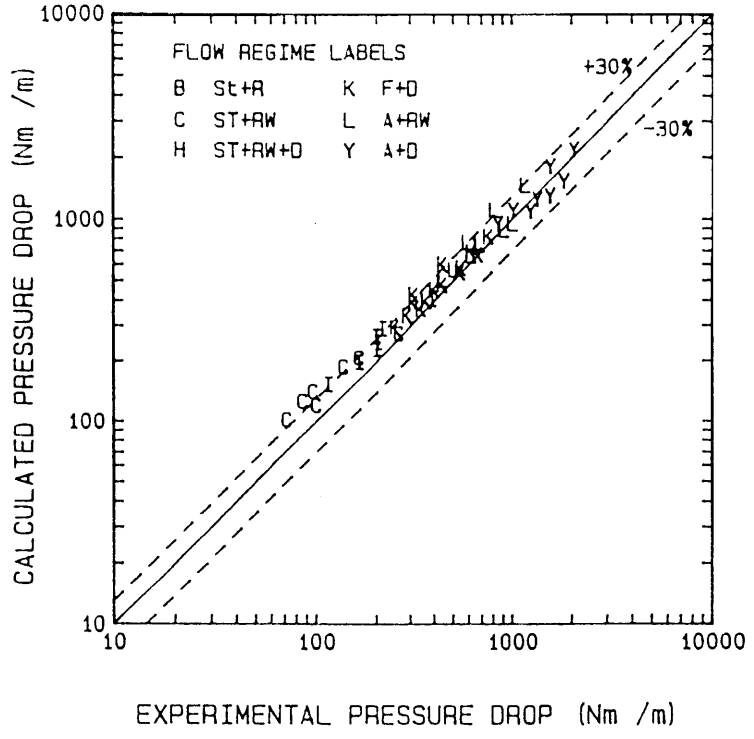

Fig. 21. Comparison between the calculated pressure drop using the Spedding–Hand [44, 45] method and experimental data from this work for $\alpha = -5$.

opposite was the case. Indeed, just above $\bar{V}_{SG} = 10$ m s^{-1}, the upward flow geometry exhibited a deep minimum in pressure loss in the blow-through-slug regime. These results have important implications for the design of two-phase pipelines which is best sloped downward and upward either side of a $\bar{V}_{SG} = 10$ m s^{-1}.

Hold-up was difficult to predict for these angles being in general flow regime dependent. The Nicklin et al. [41] model handled the bubble, slug and intermittent regimes. The Kawaji [30] and Spedding–Hand [31] models handled the stratified, stratified roll wave, stratified inertial wave and film droplet regimes while the latter model also handled the droplet and annular wave pattern. The Hart et al. [29] model predicted the stratified ripple and annular roll wave and droplet regimes. The Lockhart–Martinelli [37] theory handled blow-through-slug regimes. The Spedding–Chen [39] model handled annular blow-through-slug, annular wave and droplet regimes. Since the Hart et al. [29] model was only valid for low liquid flows the requirement for prediction of the stratified ripple regime was met by both the Spedding–Hand [44] model and a new correlation.

Pressure drop was successfully predicted for these angles using the Spedding–Hand [44, 45] model. Despite this success the hold-up was not successfully predicted by the model for the inclined data.

References

[1] M.E.G. Ferguson, P.L. Spedding, Drag reduction in two-phase gas-liquid flow, Devel. Chem. Eng. Min. Process 4 (1996) 183–96.

[2] H.D. Beggs, J.P. Brill, A study of two-phase flow in inclined pipes, J. Pet. Tech. 25 (1973) 607–17.

[3] H. Mukherjee, J.P. Brill, Liquid hold-up correlations for inclined two-phase flow, J. Pet. Tech. 35 (1983) 1003–8.

[4] H. Mukherjee, J.P. Brill, Empirical equations to predict flow patterns in two-phase flow, Int. J. Multiphase Flow 11 (1985) 299–315.

[5] P.L. Spedding, V.T. Nguyen, Regime maps for air–water two-phase flow, Chem. Eng. Sci. 35 (1980) 779–93.

[6] P.L. Spedding, J.J.J. Chen, V.T. Nguyen, Pressure drop in two-phase gas–liquid flow in inclined pipes, Int. J. Multiphase Flow 8 (1992) 407–31.

[7] P.L. Spedding, J.J.J. Chen, Hold-up in two-phase flow. Int. J. Multiphase Flow 10 (1984) 307–39.

[8] S.L. Kokal, J.F. Stanislav, An experimental study of two-phase flow in slightly inclined pipes, I Flow patterns. II Liquid hold-up and pressure drop. Chem. Eng. Sci. 44 (1989) 655–79, 681–93.

[9] P.L. Spedding, M.E.G. Ferguson, Data on horizontal and inclined $\pm 5^{\circ}$, co-current, two phase gas–liquid flow. Queen's University, Belfast. Rept CE/1/93, 1993.

[10] P.L. Spedding, V.T. Nguyen, Data on hold-up pressure loss and flow pattern for two-phase air–water flow in an inclined pipe. Rept No 122 University of Auckland 1976.

[11] P.L. Spedding, N.D. Hand, Data on horizontal co-current, two-phase gas–liquid flows. Queen's University, Belfast. Rept CE/1/89.

[12] Y. Taitel, A.E. Dukler, A model for predicting flow regime transitions in horizontal and near horizontal gas–liquid flow, AIChE J. 22 (1976) 47–56.

[13] N. Andritos, T.J. Hanratty, Interfacial instabilities for horizontal gas–liquid flow pipelines, Int. J. Multiphase Flow 13 (1987) 583–603.

[14] H. Jeffreys, On the formation of waves by wind, Proc. Royal Soc. 107(A) (1925) 189–205.

[15] J. Weisman, D. Duncan, J. Gibson, J. Crawford, Effects of fluid properties and pipe diameter on two phase flow pattern in horizontal lines, Int. J. Multiphase Flow 5 (1979) 437–462.

[16] D. Barnea, Y. Taitel, Flow pattern transition in two-phase gas–liquid flows, in: N.P. Cheremisinoff, editor. Encyclopedia of fluid mechanics. Vol. 3. Gulf, 1986. p. 403–74.

[17] D. Barnea, A unified model for predicting flow pattern transitions for the whole range of pipe inclinations, Int. J. Multiphase Flow 13 (1987) 1–14.

[18] P.Y. Lin, T.J. Hanratty, The effect of pipe diameter on flow patterns for air–water flow in horizontal pipes, Int. J. Multiphase Flow 13 (1987) 549–563.

[19] M. Ishii, M.A. Grolmes, Inception criteria for droplet entrainment in two-phase co-current film flow, AIChE J. 21 (1975) 308–317.

[20] M. Ishii, Wave phenomena and two-phase flow instabilities, in: G. Hestioni, editor. Handbook of multiphase systems. McGraw-Hill, 1982. pp. 102–104.

[21] J.E. Kowalski, Wall and interfacial shear stress in stratified flow in a horizontal pipe, AIChE J. 32 (1987) 274–91.

[22] P.L. Spedding, N.P. Hand, Prediction of hold-up and frictional pressure loss in two-phase horizontal and downward, co-current flow. Proceedings of International Symposium on Two-phase Modelling and Experimentation, Rome, 1995. p. 573–582.

[23] P.L. Spedding, N.P. Hand, M.E.G. Ferguson, Prediction of hold-up in two-phase gas–liquid vertical downflow. Proceedings of International Symposium on Two-phase Modelling and Experimentation. Rome, 1995. p. 191–6.

[24] P.L. Spedding, D.R. Spence, Prediction of hold-up two-phase flow, Int. J. Eng. Fluid Mech. 1 (1988) 67–82.

[25] P.L. Spedding, D.R. Spence, Prediction of hold-up in two-phase flow, Int. J. Eng. Fluid Mech. 2 (1989) 109–118.

[26] P.L. Spedding, K.D. O'Hare, D.R. Spence, Prediction of hold-up in two-phase flow, Int. J. Eng. Fluid Mech. 2 (1989) 369–402.

[27] P.L. Spedding, D.R. Spence, N.P. Hand, Prediction of hold-up in two-phase gas–liquid inclined flow, Chem. Eng. J. 45 (1991) 55–74.

[28] P.L. Spedding, N.P. Hand, Prediction of hold-up in two-phase gas–liquid downward inclined flow, Int. J. Eng. Fluid Mech. 5 (1992) 55–76.

[29] J. Hart, P.J. Hamersma, J.M. Fortuin, Correlations predicting frictional pressure drop and liquid hold-up during horizontal gas–liquid pipe flow with a small liquid hold-up, Int. J. Multiphase Flow 15 (1989) 947–64.

[30] M. Kawaji, Y. Anoda, H. Nakamura, T. Tasaka, Phase and velocity distribution and hold-up in high pressure steam/water stratified flow in a large diameter horizontal pipe, Int. J. Multiphase Flow 13 (1987) 135–59.

[31] P.L. Spedding, N.P. Hand, Prediction of hold-up and frictional pressure loss in two-phase co-current flow, in: Cheremisinoff, NP, editor. Encyclopedia of Fluid Mechanics Supplement 3. Gulf, 1994. p. 17–29.
[32] Y. Taitel, A.E. Dukler, A theoretical approach to the Lockhart–Martinelli correlation for stratified flow, Int. J. Multiphase Flow 2 (1976) 591–5.
[33] D. Chisholm, Two-phase flow in pipelines and heat exchangers. London: Goodwin, 1983.
[34] D. Chisholm, A.D.K. Laird, Two-phase flow in rough tubes, Trans. ASME 80 (1958) 276–86.
[35] J.J.J. Chen, A further examination of void fraction in annular two-phase flow, Int. J. Heat Trans. 29 (1986) 1760–63.
[36] H. Nishino, Y. Yamazaki, A new method of evaluating steam volume fractions in boiling systems, J. Soc. Atom Energy Japan 5 (1963) 39–46.
[37] R.M. Lockhart, R.L. Martinelli, Proposed correlation of data for thermal two-phase two-component flow in pipes, CEP 45 (1949) 29–48.
[38] G.A. Hughmark, Hold-up in gas–liquid flow, CEP 58 (1962) 62–5.
[39] P.L. Spedding, J.J.J. Chen, Hold-up in two-phase flow, Int. J. Multiphase Flow 10 (1984) 307–39.
[40] T.M. Turner, G.B. Wallis, The separate-cylinder model of two-phase flow. Report NY O311406. Thayer School of Engineering, Dartsmouth College, 1965.
[41] D.J. Nicklin, J.O. Wilks, J.F. Davidson, Two-phase flow in vertical tubes, Trans. Inst. Chem. Eng. 40 (1962) 61–8.
[42] R.H. Bonnecaze, W. Erskine, E.J. Greskovich, Hold-up and pressure drop for two-phase slug flow in inclined pipelines, AIChE J. 17 (1971) 1109–13.
[43] Z. Rouhani, Modified conditions for void and two-phase pressure drop. Report AE-RTV-841, 1969.
[44] P.L. Spedding, N.P. Hand, Prediction of hold-up and pressure loss from the two-phase momentum balance for stratified type flows. ASME "Advanced in gas–liquid flow". Editors J.S. Kim, V.S. Rohatgc, A. Hashemi, Fed 99, HTD 155 (1990) 73–88.
[45] N.P. Hand, P.L. Spedding, Stratified type gas–liquid co-current flow in horizontal pipelines, Int. J. Heat Mass Transfer 40 (1997) 1923–35.
[46] L.R. Vermuelin, J.T. Ryan, Two-phase slug flow in horizontal and inclined tubes, Can. J. Chem. Eng. 49 (1971) 195–202.
[47] L. Mattar, G.A. Gregory, Air–oil slug flow in an upward-inclined pipe I slug velocity, hold-up and pressure gradient, J. Can. Pet. Tech. January–March (1974) 69–76.
[48] M.E.G. Ferguson, P.L. Spedding, Measurement and prediction of pressure crop in two-phase flow, J. Chem. Tech. Biotechnol. 62 (1995) 262–78.
[49] Z. Olujic, Predicting two-phase flow friction loss in horizontal pipes, Chem. Eng. 24 (1985) 45–50.